

# Inertial microfluidics

Dino Di Carlo\*

Received 25th June 2009, Accepted 19th August 2009

First published as an Advance Article on the web 22nd September 2009

DOI: 10.1039/b912547g

Despite the common wisdom that inertia does not contribute to microfluidic phenomena, recent work has shown a variety of useful effects that depend on fluid inertia for applications in enhanced mixing, particle separation, and bioparticle focusing. Due to the robust, fault-tolerant physical effects employed and high rates of operation, inertial microfluidic systems are poised to have a critical impact on high-throughput separation applications in environmental cleanup and physiological fluids processing, as well as bioparticle focusing applications in clinical diagnostics. In this review I will discuss the recent accelerated progress in developing prototype inertial microfluidic systems for a variety of applications and attempt to clarify the fundamental fluid dynamic effects that are being exploited. Finally, since this is a nascent area of research, I will suggest some future promising directions exploiting fluid inertia on the microscale.

## Introduction

Traditionally, microfluidics has often been associated with negligible inertia. That is, fluid flow in microfluidic channels is assumed to occur at low Reynolds number, where Reynolds number ( $Re = \rho UH/\mu$ ) is a dimensionless parameter describing the ratio between inertial and viscous forces in a flow. This assumption is arrived at because microchannel dimensions,  $H$ , are small ( $<1$  mm). However, for water with density,  $\rho \sim 1000$  kg/m<sup>3</sup> and viscosity,  $\mu \sim 0.001$  Pa s, in a channel with a diameter of 100  $\mu$ m, the Reynolds number of the flow approaches 1 for a low

mean flow velocity,  $U$  of  $\sim 0.01$  m/s. For this relatively common case, neglecting inertia by using a Stokes flow (*i.e.*  $Re = 0$ ) approximation can lead to incorrect results. Steady-state Stokes flow is arrived at by setting the left hand side (*i.e.* inertial components “ $ma$ ”) of the Navier–Stokes equations, which describe the balance of linear momentum for a Newtonian fluid:  $\rho(\partial \mathbf{u}/\partial t + \mathbf{u} \cdot \nabla \mathbf{u}) = -\nabla p + \mu \nabla^2 \mathbf{u} + \mathbf{f}$ , to zero. Here  $\mathbf{u}$  is the fluid velocity field,  $p$  is the pressure field, and  $\mathbf{f}$  is a vector field of external body forces acting on fluid elements. Stokes flow is often incorrectly equated with laminar flow, but these are separate concepts – Stokes flow implies laminar flow, but the opposite is not necessarily true. It is true that in all but the most extreme cases, flows in microchannels are laminar and predictable since turbulence is usually observed for  $Re > \sim 2000$ <sup>1</sup> (20 m/s average velocity in our previous example!). Here I focus on an often neglected middle regime where both inertia and viscosity of the fluid are finite, between Stokes flow and inviscid flow, where the solutions to the full Navier–Stokes equations are required.

Several inertial effects are beginning to see use in microfluidic systems. The predominantly used effects that I will focus discussion on are: (1) secondary flows in curved channels, and (2) inertial migration of particles. Geometry-induced re-circulating flows that become significant with finite inertia have also briefly been explored for microfluidic applications<sup>2,3</sup> but will not be discussed here because theory and experimental results for these systems are less well developed. In the following sections I will begin by generally discussing the physical bases for the two main effects and review how they have been exploited in microfluidic environments for specific applications. I will concurrently discuss the advantages and disadvantages of inertial microfluidic approaches and conclude with future directions that appear promising.

## Secondary flow in curved channels

Improved mixing and precise control over fluid interfaces can be achieved by utilizing flows transverse to downstream fluid streamlines in curved channels. Key external parameters to

Department of Bioengineering and California NanoSystems Institute, Henry Samueli School of Engineering and Applied Science, University of California, Los Angeles, CA, 90095. E-mail: dicarlo@seas.ucla.edu



Dino Di Carlo

Dino Di Carlo is an Assistant Professor in the Department of Bioengineering at the University of California, Los Angeles where he leads the Microfluidic Biotechnology Laboratory ([www.biomicrofluidics.com](http://www.biomicrofluidics.com)). He received his BS in Bioengineering from the University of California, Berkeley in 2002 and received a PhD in Bioengineering from the University of California, Berkeley and San Francisco in 2006 in Luke Lee's BioPOETS Lab. He then conducted postdoctoral studies from 2006–2008 at the Center for Engineering in Medicine at Harvard Medical School and Massachusetts General Hospital under the guidance of Mehmet Toner. His research focuses on exploiting unique physics, microenvironment control, and the potential for automation associated with miniaturized systems for applications in basic biology, medical diagnostics, and cellular engineering.

He then conducted postdoctoral studies from 2006–2008 at the Center for Engineering in Medicine at Harvard Medical School and Massachusetts General Hospital under the guidance of Mehmet Toner. His research focuses on exploiting unique physics, microenvironment control, and the potential for automation associated with miniaturized systems for applications in basic biology, medical diagnostics, and cellular engineering.

control these flows include the *channel dimensions*, *radius of curvature*, and *flow rate*.

### Physics of Dean flow

Secondary flow arises in fluid flow through a curved channel because of a mismatch of velocity in the downstream direction between fluid in the center and near-wall regions of a channel. Therefore, fluid elements near the channel centerline have larger inertia than fluid near the channel walls, and would tend to flow outward around a curve, creating a pressure gradient in the radial direction of the channel. Because the channel is enclosed, relatively stagnant fluid near the walls re-circulates inward due to this centrifugal pressure gradient, creating two symmetric vortices (Fig. 1). A dimensionless number that describes the magnitude of this flow was first established by W. R. Dean, and a more generally accepted form of this Dean number is described by Berger *et al.*<sup>4</sup> as  $\kappa = (H/2R)^{1/2} Re$ . Berger *et al.* noted that, although not explored, the ratio of channel dimension to radius of curvature, defined by the parameter  $\delta = H/(2R)$ , also has important effects on the shape of the secondary flow.<sup>4</sup> Following Squires and Quake<sup>1</sup> the secondary flow velocity scales as  $U_D \sim \kappa^2 \mu/(\rho H)$ . Besides giving a measure of the Dean flow velocity, increases in Dean number are associated with changes in shape of the secondary flow, with the centers of the symmetric vortices moving towards the outer wall and development of boundary layers with increasing  $\kappa$ .<sup>4</sup>

### Applications of secondary flow in microfluidic systems

Secondary flows have been employed in microfluidic systems primarily for applications in fluid mixing. Mixing in microfluidic systems has been extensively explored because of the difficulty in quickly mixing fluid streams without the aid of turbulence (reviewed in ref. 5 and articles in that issue of *Philosophical Transactions*). Most techniques are based on the concept of increasing the interfacial area for diffusive mixing to occur. Often the concept of chaotic advection is used, whereby fluid interfaces are stretched and folded to increase the interfacial area to an extreme level.<sup>6</sup> Because of the exponential growth in stretching of fluid interfaces in these systems the positions of individual fluid elements cannot be confidently assigned, recapitulating an aspect of turbulent flow that leads to good mixing.

Secondary flows in curved microfluidic channels have been used to increase the interfacial area for diffusive mixing. One of the first examples is the use of three-dimensional “twisted” channels analogous to macroscale systems that take advantage of chaotic advection.<sup>7</sup> In this work, Beebe *et al.* observed almost complete mixing for  $Re < 25$ , which was a significant improvement over a planar serpentine channel in which Dean flow stretched interfaces symmetrically back and forth with each turn, therefore not yielding chaotic advection. Ligler *et al.* demonstrated a circular curve design that stretches fluid streams in a single direction to increase mixing efficiency.<sup>8</sup> Alternative designs have been demonstrated by Sudarsan and Ugaz using spiral channels (Fig. 2A), and further improvements employed curved channels to reorient fluid elements followed by branching channels that separately reoriented and recombined fluid elements, creating aspects of chaotic advection.<sup>2,9</sup> In these single-

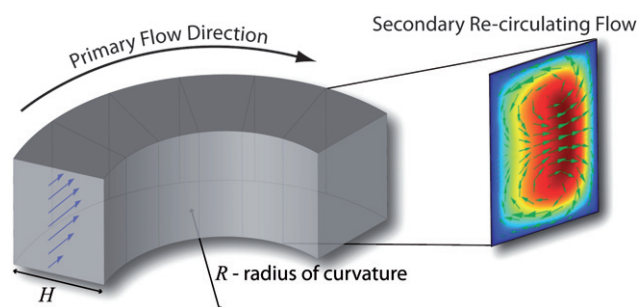


**Fig. 1** Dean flow. In curved channels, when inertia is important, faster moving fluid near the channel center tends to continue outward, and to conserve mass, more stagnant fluid near the walls re-circulates inward. This creates two counter-rotating vortices perpendicular to the primary flow direction.

layer systems effective mixing of a fluorescent dye was achievable for  $Re > 20$ . Advantages of using secondary flow in curved channels for mixing include: (i) the relatively simple design and operation, (ii) enhancement of mixing with increasing flow rate as opposed to diffusive mixing, and (iii) applicability to a range of different fluids of varying viscosities, densities, and conductivities. However, it should be noted that these techniques are often not appropriate for many Lab-on-a-Chip applications dealing with small volumes of fluid, since mixing enhancement becomes negligible for lower flow rates where  $\kappa < \sim 1$ .

Besides mixing, the ability to controllably deform the interface between two co-flowing fluids has been employed for other applications. Huang *et al.* used the two re-circulating vortices in Dean flow to transform vertically co-flowing streams into horizontal co-flowing streams (Fig. 2B). Additional fluid inputs were then added to pinch the horizontal streams creating a 3D hydrodynamic focusing effect in a single-layer microfluidic chip.<sup>10</sup> If instead of completely transforming the co-flow to horizontal, the interface between the two co-flowing streams is slightly deformed then the curvature that is created can be used as an optical lens if the two fluids have different indices of refraction<sup>11</sup> (Fig. 2C). Huang *et al.* demonstrated a tunable lens using the co-flow of calcium chloride solution and deionized water.<sup>11</sup> Here the focal length of the lens was tunable by adjusting the flow rate (*i.e.* Dean flow velocity) through the curved channel.

Dean vortices have also been used to act on particles in flow. Go *et al.* separated particles with significantly higher density than the fluid based on the idea that larger particles intercept different secondary flow velocity fields than smaller particles, leading to differential movement (Fig. 2D).<sup>12</sup> Caveats to interpretation of the results of this work include the need to consider inertial lift forces acting on particles, and the effect of large particles on distorting the secondary flow field itself. In fact, the interaction of inertial lift forces with secondary Dean flows leads to complex and useful behavior – as discussed below.

### Inertial migration of particles

Parallel and precise cell and particle manipulation can be achieved using inertial lift forces intrinsic to particle motion in confined channel flows. Key external parameters to control the

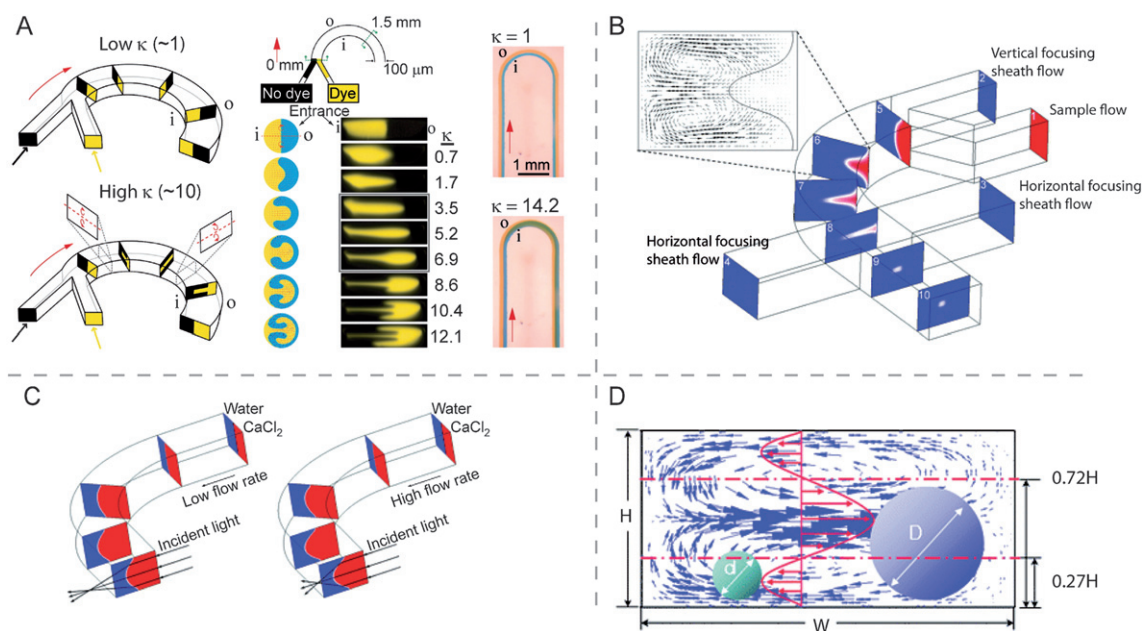


**Fig. 2** Applications of secondary flow in curved channels. (A) Dean flow was used to increase the interfacial area for diffusive mixing in microchannels. Image printed with permission from Ugaz *et al.*<sup>2</sup> (B) 3-D hydrodynamic focusing of fluid streams in a single layer system was achieved by rotating the initial stream in a Dean flow prior to pinching the flow again. Image printed with permission from Huang *et al.*<sup>10</sup> (C) Similarly, a variable focal length lens was created by inertial modulation of the curvature between two co-flowing streams with different refractive indices.<sup>11</sup> (D) Larger particles will intersect different regions of the secondary flow velocity field, which leads to separation.<sup>12</sup>

magnitude and direction of lift forces include the *channel dimensions & aspect ratio, particle diameter, and flow rate.*

### Physics of inertial migration

Particles in a flow experience both shear and normal stresses acting over their surfaces that yield forces parallel (*i.e.* drag forces) and perpendicular (*i.e.* lift forces) to the main flow direction. In most flows, drag forces will act to accelerate particles until they are force free in the flow direction and travel at the average intersected fluid speed. Lift forces are most often associated with inviscid, unbounded flows acting on “particles” (*e.g.* wings) of defined shape. Lift on particles within bounded channel flows has been less studied presumably because both viscous and inertial components are important in these flows. Simple physical explanations for the processes yielding lift forces are often hard to come by, with a significant example being that one of the most common intuitive arguments for lift on an airplane wing is considered flawed (*i.e.* the equal transit time argument). In any case, studies have led to significant insight into scaling and necessary factors required for these forces.

Migration of rigid particles (due to lift) across undisturbed streamlines was first reported in the 1960s for macroscale flows through a cylindrical pipe.<sup>13</sup> Segre and Silberberg observed that randomly dispersed millimeter-diameter particles migrated to an annulus centered at a position  $\sim 0.6$  times the radius of a 1 cm diameter pipe (Fig. 3A). At the time this phenomenon was not explained by fluid dynamic theory, partly because of the difficulty of analytical calculations when the Reynolds number is finite and inertia is important (in the cylindrical-pipe experiments, Reynolds numbers between 1–100 were used). Following the observations of Segre and Silberberg a flurry of theoretical

investigations ensued in an attempt to capture this unique behavior. The technique of matched asymptotic expansions proved to be one of the most useful for determining dominant lateral forces on particles of diameter,  $a$ , in channels of dimension,  $H$ , and yielded a lift force,  $F_L$ , that scales as:  $F_L \propto \rho U^2 a^4 / H^2$ .<sup>14–18</sup>

Besides yielding a scaling for the lift, theoretical investigations into inertial migration of particles have identified the dependence of lift on cross-sectional position within a channel,<sup>15–18</sup> showed an additional dependence of lift on  $Re$ ,<sup>16–18</sup> and relaxed constraints on analytical solutions requiring low values of  $Re$ .<sup>16–18</sup> A main success of the developed theory is that the dependence of the lift force on the cross-sectional position in the channel (as depicted in Fig. 3D) recapitulated the experimentally observed equilibrium position at  $\sim 0.6$  times the channel radius.<sup>15–18</sup> Here, and throughout this work, the definition of “equilibrium” or “equilibrium positions” does not imply that the system is at equilibrium in the thermodynamic sense, but rather implies the mathematical definition that particles occupy a stationary point of a dynamical system. Further dependence of lift force on channel Reynolds number was also theoretically predicted, such that  $F_L = f_L(Re, x/h) \cdot \rho U^2 a^4 / H^2$  where  $f_L$  is a non-dimensional lift coefficient that is a function of Reynolds number and the normalized cross-sectional position ( $x/h$ ).<sup>16–18</sup> Interestingly,  $f_L$  has been shown to decrease with increasing  $Re$  or  $U$  suggesting that lift scales slightly less strongly than with  $U^2$ .<sup>16–18</sup> These previous investigations also found that similar forms of the lift force were observed for cylindrical channels<sup>14,18</sup> and parallel plates.<sup>15–17</sup> For all of the work using matched asymptotic expansions, an assumption of small particle Reynolds number ( $R_p = Re(a/H)^2 = \rho U a^2 / H$ ) and  $a/H \ll 1$  was used such that the particle does not disturb the underlying flow field. Here the



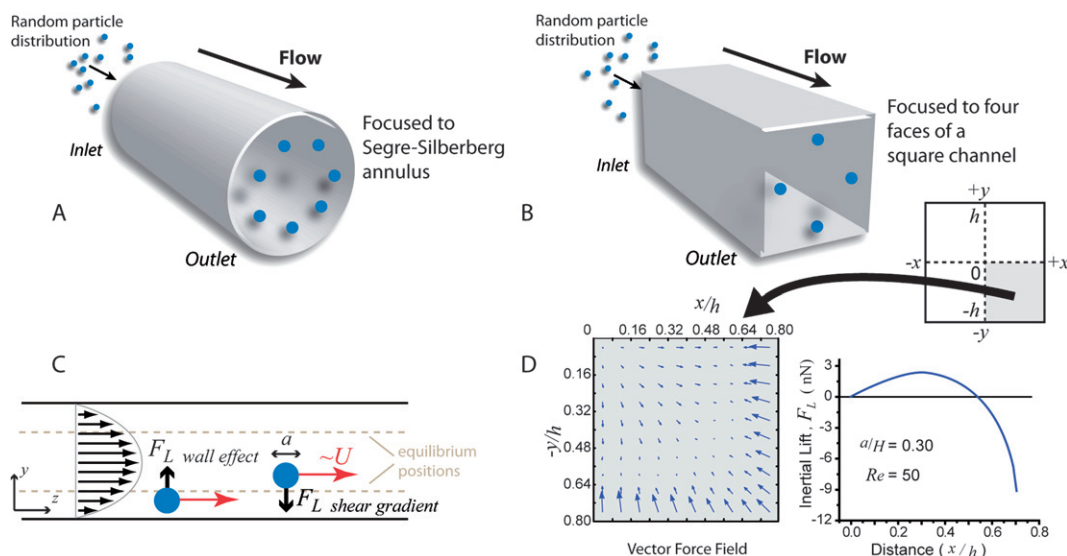


**Fig. 3** Inertial lift. (A) In a cylindrical pipe, at moderate Reynolds numbers, randomly distributed particles are known to focus to an annulus located between the center and wall of the pipe. (B) In square channels, following the symmetry of the system, particles instead focus to four equilibrium regions centered at the faces of the channels for dilute suspensions of particles flowing at moderate Reynolds numbers. (C) Two lift forces perpendicular to the flow direction act to create equilibrium positions in channels, (i) a “wall effect” lift that is directed away from the wall and decays with distance from the wall and (ii) a shear gradient lift that is directed down the shear gradient and is zero at the channel centerline. Interaction of the two forces leads to defined equilibrium positions in channel flows. (D) In square channels, the simulated force field on a particle over a fourth of a channel cross-section is shown.<sup>19</sup> A plot of the magnitude of inertial lift forces at  $y = 0$  is also shown demonstrating the general shape of the combined shear-gradient and wall-effect lift and magnitudes in the nano-newtons for the labeled conditions (15  $\mu\text{m}$  particle in a 50  $\mu\text{m}$  channel,  $Re = 50$ ).

particle Reynolds number is a measure of the ratio of inertial to viscous forces of the disturbance from the underlying channel flow at the *particle length scale* and contrasts with a particle Reynolds number dependent only on length dimensions of the particle in an unbounded flow.

Recently, myself and others have shown that some aspects of particle migration in these confined geometries cannot be predicted using these assumptions – such that the finite-size of the particle plays an important role in inertial migration when  $a/H$  is of order 1.<sup>19,20</sup> Finite element solutions to the complete incompressible Navier–Stokes Equations yielded a novel scaling for the lift force in this case that was further dependent on a particle’s position in the channel.<sup>19</sup> Our work showed that lift scaled as  $F_L \propto \rho U^2 a^3/H$  near the channel centerline, but scaled instead as  $F_L \propto \rho U^2 a^6/H^4$  near the channel wall. Differences in scaling between the channel wall and centerline suggest two disparate fluid dynamic effects physically act to create inertial lift equilibrium positions. Ho and Leal, and Matas *et al.* discussed two components of inertial lift that together act to yield an equilibrium position between the channel wall and centerline:<sup>15,18</sup> (1) a “wall effect” lift that is always away from the wall towards the channel centerline, and (2) a “shear-gradient” lift that acts down the gradient in shear rate of the flow (Fig. 3C). Note that a gradient in shear rate is naturally present in Poiseuille flow (parabolic velocity profile), but not in Couette flow (linear velocity profile).

For finite-size particles, another useful parameter, the lateral particle migration velocity ( $U_p$ ) can be shown to scale with particle Reynolds number. One can calculate a migration velocity for particles near the channel centerline by balancing shear-gradient inertial lift with Stokes drag ( $F_{\text{Stokes}} = 3\pi\mu a U_p$ ). This leads to a fractional lateral migration velocity per

downstream velocity:  $U_p/U \propto R_p$ . Therefore, particles are predicted to travel a lateral distance ( $L_x$ ) towards equilibrium positions that is proportional to the particle Reynolds number and the given downstream position ( $L_z$ ):  $L_x \propto R_p L_z$ . This equation is useful to inform design decisions for inertial microfluidic systems given an assumption of an average value for the lift coefficient ( $f_L$ ) between 0.02 and 0.05 over the channel cross-section and that shear-gradient lift limits migration to equilibrium positions compared to stronger wall effect lift (see Box 1).

Focusing equilibrium positions due to inertial lift have also been shown to be dependent on channel symmetry. Particles in cylindrical channels focus to an annulus following the channel symmetry (Fig. 3A). Recently, particles flowing through square or rectangular channels were also found to focus to equilibrium positions following the 4-fold channel symmetry (Fig. 3B,D, Fig. 4A).<sup>19,21–23</sup> Interestingly, as the aspect ratio of the channel becomes larger (*i.e.* a very wide or very tall channel) focusing again follows symmetry and reduces to predominantly two equilibrium positions centered at the long face of the channel.<sup>19,24,25</sup>

In addition to lift forces creating equilibrium positions for particles within the cross section of a channel, particles suspended at intermediate densities will interact in a flow with finite inertia to create particle trains with *regular spacing in the direction of flow* (Fig. 4B).<sup>25–28</sup> This has been observed by Morris *et al.* as single trains in millimeter scale pipe flows,<sup>26</sup> and by Edd and Di Carlo as staggered “double-trains” for flows through rectangular microchannels.<sup>25</sup> Ogino *et al.* simulated cylinders flowing through infinite plates with finite  $Re$  that yielded similar staggered inter-particle coupling.<sup>28</sup>

Particle concentration is also a critical factor affecting focusing behavior and accuracy. Aside from the interparticle interactions

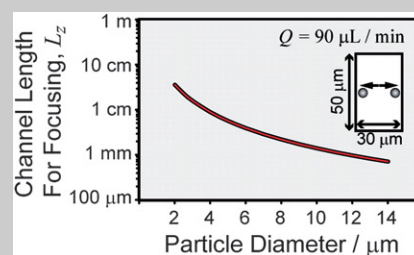
### Box 1 - Practical design rules for inertial focusing

The complexity of the forces involved in inertial focusing introduces difficulties in development of general design rules that are easily applied to any system. However, for straight rectangular channel systems we can make several assumptions to arrive at relatively simple equations that inform design decisions. Note that the accuracy of these assumptions has not been rigorously tested experimentally.

#### (1) Channel length ( $L_f$ ) required for focusing to equilibrium positions.

$$L_f = \frac{\pi\mu H^2}{\rho U_m a^2 f_L}$$

The average  $f_L$  varies from  $\sim 0.02$ – $0.05$  for aspect ratios ( $H/W$ ) from 2 to 0.5 where  $H$  is the channel width in the direction of particle migration. See inset figure for focusing lengths required as a function of particle size for a typical channel geometry and flow rate.  $\mu$  and  $\rho$  are the fluid viscosity and density,  $U_m$  is the maximum channel velocity and  $a$  is the particle diameter.



#### (2) Flow rate ( $Q$ ) required for focusing to equilibrium positions for a channel of length $L$ .

$$Q \approx \frac{2\pi\mu WH^3}{3\rho L a^2 f_L}$$

Again  $H$  is the channel dimension in the direction of particle migration, and  $W$  is the channel width in the perpendicular direction. Note that the  $2/3$  multiplier comes from the conversion of the maximum velocity to the average velocity in flow through parallel plates, and is dependent on channel aspect ratio.

#### (3) Guidelines for practical focusing in continuously curving channels.

The length and flow rate requirements should follow those described in (1) and (2), and in addition the following inequality should be satisfied:

$$R_f = \frac{a^2 R}{H^3} > 0.04$$

Where  $R$  is the largest radius of curvature in the system and  $H$  is the smallest dimension of the channel.

described above, there are steric crowding effects since particles are concentrated to a few relatively narrow streamlines. To identify when these effects occur, the number of particle diameters per channel length (or length fraction,  $\lambda$ ) can be defined, which is more useful than a volume or weight fraction given that particles are focused to single streams. One can convert from a volume fraction to this value using the following relation:  $\lambda = aV_f/V_p = 6WHV_f/\pi a^2$ , where  $V_f$  is the volume fraction of particles in the solution,  $W$  is the channel width, and  $H$  is the channel height. For  $\lambda > 1$ , focusing to a single stream cannot be expected due to steric interactions between particles. Note that for a constant volume fraction the length fraction increases significantly with decreasing particle diameter,  $a$ , such that accurate focusing of smaller particles requires quite dilute solutions. For example,  $\lambda = 1$  for  $2\ \mu\text{m}$  particles in a  $50 \times 30\ \mu\text{m}$  channel when the volume fraction is equal to the small value of 0.001.

#### Applications of inertial migration in microfluidic systems

Although the phenomenon of inertial migration has been studied for the last 40 years, commercial applications have been few. This is partly because only recently was it appreciated that inertial lift and ordering effects act and are useful in microfluidic flows<sup>21</sup> where their use may have a profound impact. There are

particularly relevant applications for cell and particle manipulation without complex fabrication and at extremely high rates. In contrast to many microfluidic devices, because inertial microfluidic systems operate at high flow rates, they are generally advantageous for macroscale operations (utilizing microscale physical principles), but are not ideal for operating on small volumes that are required for some miniaturization applications.

Applications for particle and cell separation and filtration are particularly logical given that (i) inertial lift forces scale with a power of particle size, and (ii) the ability to operate at higher flow rates is a significant advantage for most separation and filtration applications. Both kinetic separations (*i.e.* differences in migration times for particles of different sizes leads to separation,<sup>29</sup> Fig. 4D) and equilibrium separations (*i.e.* fundamental differences in equilibrium positions for particles of different sizes<sup>19</sup>) are possible using inertial lift in straight microchannels. Filtration is perhaps more simple since it requires only concentration and collection of particles into separate channels after reaching inertial lift equilibrium positions in a straight rectangular channel (Fig. 4C). Papautsky *et al.* demonstrated filtration of  $2\ \mu\text{m}$  particles from water in  $20 \times 50\ \mu\text{m}$  channels at a Reynolds number of 20 after traversing a channel length of  $\sim 4\ \text{cm}$ .<sup>23</sup> This size is similar to that of some fungi, large bacteria, and protists suggesting possible applications in water filtration. Additionally, similar high-aspect ratio channels have been shown

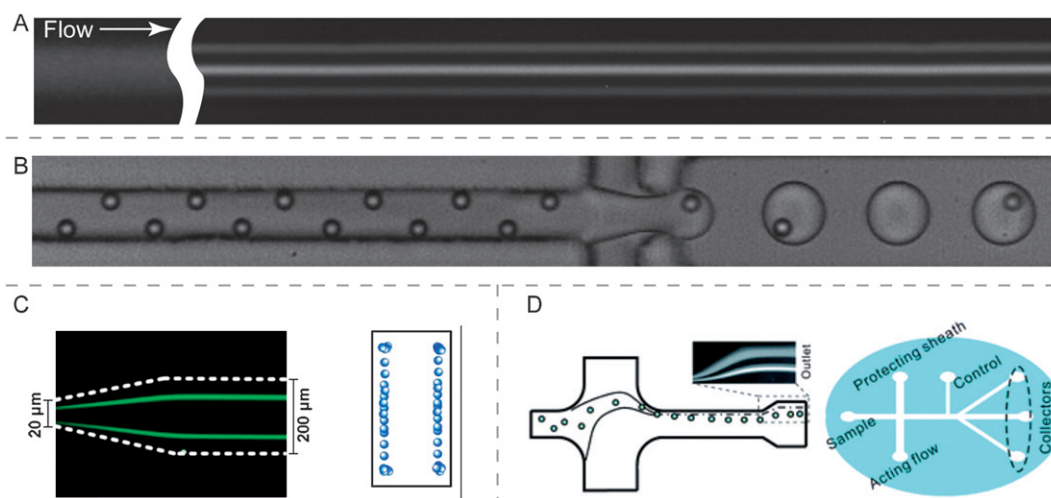


**Fig. 4** Applications of inertial migration in straight channels. (A) In a 50  $\mu\text{m}$  square channel streak images of 10  $\mu\text{m}$  particles are shown 4 cm downstream. Particles that are initially randomly distributed focus to what appears to be three streams with the brighter middle stream corresponding to two streams at different depths superimposed. Focused streams are useful for applications in flow cytometry, concentration, filtration, and separation.<sup>21</sup> (B) For high-aspect ratio channels with a height of 50  $\mu\text{m}$  and width of 27  $\mu\text{m}$ , focusing of 10  $\mu\text{m}$  particles to two streamlines is observed. Particles are observed to hydrodynamically interact and self-order into staggered “double-trains” for a particle Reynolds number  $\sim 0.2$ . The inertial self-ordering effect was utilized to create more uniform single-particle occupancy droplets if the frequency of the ordered particle stream is synchronized with droplet generation frequency in a microfluidic droplet generator.<sup>25</sup> (C) High-aspect ratio channels were used to focus smaller 2  $\mu\text{m}$  particles for filtration applications. Image printed with permission from Papautsky *et al.*<sup>23</sup> (D) Differential transport rates for two size particles due to differences in the magnitude of wall effect lift were employed for separation of blood cells ( $\sim 8 \mu\text{m}$ ) from bacteria ( $\sim 1 \mu\text{m}$ ). Image printed with permission from ref. 29.

to focus 7 and 10  $\mu\text{m}$  particles<sup>25,30</sup> and cells<sup>25</sup> to two equilibrium streams for  $R_p > \sim 0.2$ , useful for filtration and concentration applications. Although the authors discuss a separate mechanism, I would argue that Hjort *et al.* have also demonstrated kinetic separations, whereby hydrodynamic focusing of a mixed blood cell/bacteria stream against a wall, allowed for migration of larger blood cells away from the wall at a faster rate than smaller bacteria (Fig. 4D).<sup>29</sup> This system allowed for high-purity separation of *E. coli* from red blood cells with throughputs up to 18  $\mu\text{L}/\text{min}$ . Parallelization for further improvements in throughput with this platform is a future challenge because of the multiple fluid inputs required for the initial hydrodynamic focusing step.

It should be noted that inertial lift forces were recognized to play a role in particle behavior in field flow fractionation (FFF) based separations pioneered by J. Calvin Giddings *et al.*<sup>31–33</sup> and were briefly explored in the early 1990's. Applications or commercial instruments employing inertial lift and arising from these investigations are not apparent. Additionally, Bellhouse *et al.* proposed using inertial lift force (particularly lift away from walls) in combination with cross-flow filtration with traditional filters for size based separations.<sup>34</sup>

### Inertial migration in curved channels

Particles flowing in curving channels with finite inertia will experience both inertial migration and influences from secondary Dean flow. For most cases, where particles are relatively neutrally buoyant, centrifugal effects on the suspended particles themselves appear negligible.<sup>35</sup> A combination of Dean flow and inertial lift can provide precise focusing and positioning of particles for applications in concentration and separation. Key external parameters to control particle focusing behavior include

the channel dimensions, aspect ratio and radius of curvature, particle diameter, and flow rate.

### Physics of inertial migration in curved channels

For particles flowing in curved channels, as a first order approximation, one can make an assumption that the effects of inertial migration and secondary flow act in superposition on a particle<sup>21</sup> (Fig. 5). This is such that a particle held stationary at an inertial lift equilibrium position will experience a drag force that at its maximum will be directly proportional to the local secondary flow velocity field ( $U_D$ ) – perpendicular to the primary flow direction. This “Dean drag” force then acts to entrain particles in the secondary flow in competition with lift forces directed towards inertial lift equilibrium positions. We proposed that a ratio of these forces (*inertial lift/Dean drag*) would be a key parameter describing behavior in these systems<sup>21,36</sup> with recent evidence supporting this claim.<sup>35</sup> An inertial force ratio,  $R_f = a^2 R/H^3$  that describes the order of magnitude scaling between these forces, is obtained by dividing the dimensional scaling of inertial lift in the shear gradient region<sup>19</sup> with the scaling of Dean drag, neglecting any position and  $Re$ -dependent changes.<sup>35</sup> This dimensionless group is useful for predicting particle behavior, as demonstrated by the two limiting cases: (i)  $R_f \rightarrow 0$ , particle streams will neglect inertial equilibrium positions and remain entrained in the secondary flow, and (ii)  $R_f \rightarrow \infty$ , for sufficiently high particle Reynolds number, particles will migrate to inertial focusing equilibrium positions independent of the secondary flow. The most interesting case, for intermediate  $R_f$ , inertial equilibrium positions can be modified by the secondary flow leading to interesting new focusing modes and applications (Fig. 5). Our recent results suggest that this intermediate range starts at  $R_f > \sim 0.04$ .<sup>35</sup> Notice that  $R_f$  is dependent on particle

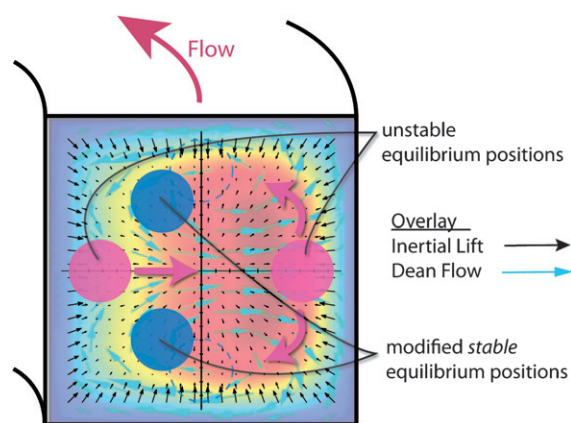


**Fig. 5** Superposition of inertial lift and Dean flow in curved channels. Inertial lift force vectors (blue) are superposed with Dean flow velocity vectors (green) for a square channel. Presumed stable and unstable equilibrium positions are indicated based on previous experimental results. Stable focusing positions in straight channels are shown as red solid circles and blue dashed circles.

size, such that two particles can experience different behavior in a channel with the smaller particle becoming entirely entrained in the secondary flow while the larger particle is focused at inertial equilibrium positions. Given that  $R_f$  is a global parameter of the system, and that inertial lift and Dean drag will vary across the channel cross-section as well, a different situation arises for two closely sized particles where lift and drag balance at two different locations within the channel cross-section, with potential uses for continuous separations. Although  $R_f$  provides a parameter to help simplify use of these systems (see Box 1), the exact mechanism and location of superposition of secondary flow and lift effects is complex and unknown experimentally and theoretically, such that I currently can only speculate in Fig. 5 on the precise combined behavior.

### Applications of inertial migration in curving microfluidic systems

Because of additional fluid dynamic forces present in curving channels, additional applications in filter-less separation and particle focusing are theoretically possible and have been demonstrated. For square or near-square channels reduced focusing to a smaller number of equilibrium positions is observed in curving channels due to the influence of secondary Dean flow<sup>21,37</sup> with applications in focusing and filtration (Fig. 5 and 6). Interestingly, for high-aspect ratio geometries (*i.e.* width  $\gg$  channel height) focusing to a reduced number of equilibrium positions is possible *without curvature*<sup>19,35</sup> with equilibrium positions roughly corresponding to those in high aspect ratio curving channels.<sup>36,38–40</sup> Nevertheless, it appears that there are separate advantages gained from adding curvature including: (i) movement of the equilibrium streamlines away from the channel centerline for improved collection capability, and (ii) reduction in channel length, and thus power, required for focusing due to the mixing action of the secondary flow allowing particles to bypass low lift force regions in the channel.<sup>35</sup> (iii) Additionally, curved channels allow for equilibrium separations based on different inertial force ratios,  $R_f$ , for different size particles.<sup>36,39</sup>

Specific curving geometries have been employed for filtration and separation applications including spirals,<sup>38–40</sup> single curves,<sup>35,37</sup> and symmetric and asymmetric serpentine curves.<sup>21,36</sup> Spiral microchannels are most common and have been used by Papautsky *et al.*<sup>39</sup> for separation of polystyrene particles of 2 and 7  $\mu\text{m}$  in size (Fig. 6A) and by Seo *et al.* from Palo Alto Research Center (PARC)<sup>38</sup> for particle filtration (Fig. 6B). The work at PARC is perhaps the most commercially developed, with scale up of their spiral separation system to 100 L/min through parallel stacking of disk-like filtration units.<sup>41</sup> Their work suggests promising applications in membrane-free, low maintenance, wastewater clarification, pre-treatment for desalination plants, and industrial liquid filtration. In current work, spiral designs have not been optimized based on physical principles, so I anticipate that improved, smaller foot-print, lower power- consumption designs are possible and should be explored. For example, Oozeki *et al.* showed flow of particles in a single curved channel of radius of curvature 20 mm spanning 180° lead to focusing to one streakline slightly off-center and towards the outer wall (Fig. 6C).<sup>37</sup> Notably, in this work channels were nearly square and results contrast with those from high-aspect ratio spiral channels in which focusing was observed near the inner channel wall.<sup>38,39</sup> Together, these data suggest that the distance from the inner wall for the focused streams in curving channels will depend strongly on channel aspect ratio (*i.e.*  $W/H$ ), with the focusing positions moving inwards with increasing aspect ratio. In fact, Papautsky *et al.*<sup>42</sup> recently confirmed this observation by demonstrating that focused particle streams moved towards the inner wall of spiral channels with increasing aspect ratio while maintaining  $\kappa$  constant. Both Papautsky *et al.*<sup>42</sup> and Russom *et al.*<sup>43</sup> also recently demonstrated that in spiral channels, particles of different sizes focused to different lateral positions within the channel cross-section as predicted considering slight differences in the local ratio of inertial lift to Dean drag for different size particles. An advantage of these approaches is continuous separation of particles of multiple sizes in a single pass, which was not achievable previously. A drawback of spiral or curved channels that turn in only one direction is that it is difficult to place many of these systems in parallel on a single substrate.

Serpentine curved channels that alternate turning direction are more easily parallelized, and by introducing asymmetry in the curvature (through different widths or radii of curvature) focusing similar to spiral channels can be achieved (Fig. 6D).<sup>21,35</sup> Parallel focusing is of potential use for ultra high-throughput flow cytometers that do not require sheath fluids given that a sufficiently parallel optical or electrical interrogation method is employed. Encouraging for applications in flow cytometry, several studies have demonstrated that cells are not significantly affected by the high flow and shear rates in inertial microfluidic systems.<sup>21,25,36,42</sup> This is because cells are not stationary on a surface, but move and rotate force free with the fluid without significant deformation (*i.e.* high shear rates are accompanied by high rotation rates that consequently minimize the shear stress acting on cells). We have also used asymmetrically curved channels for equilibrium separation, taking advantage of differences in  $R_f$  for different size particles to selectively enrich larger particles at inertial focusing positions (Fig. 6E).<sup>36</sup> Platelets were



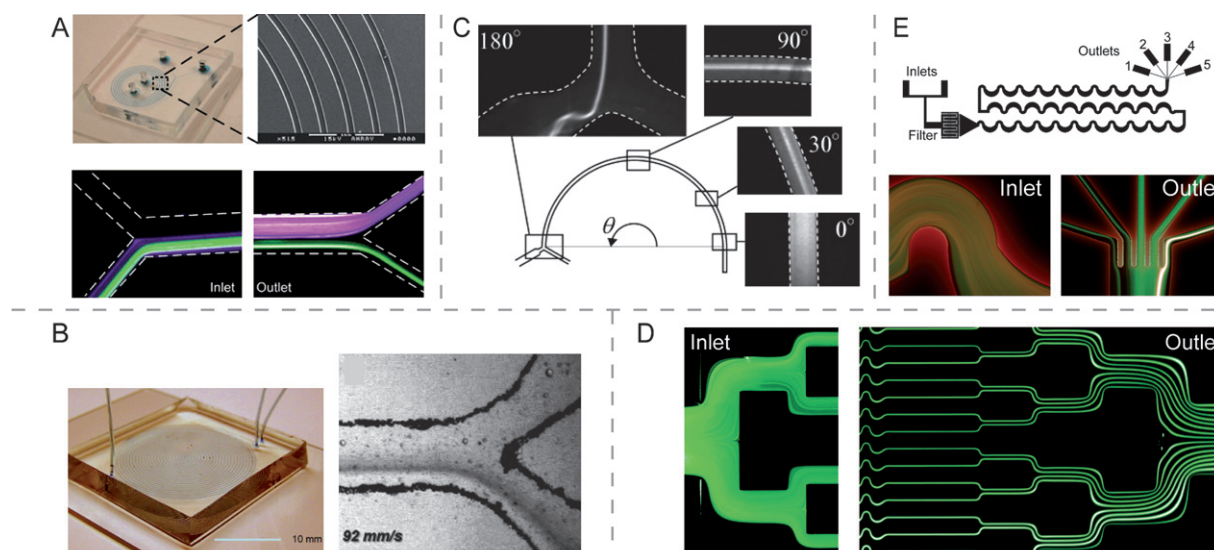


**Fig. 6** Applications of inertial migration in curved channels. (A) Complete separation of populations of particles ( $7\ \mu\text{m}$  and  $2\ \mu\text{m}$ ) is demonstrated using spiral channels with two inlets and two outlets due to differences in the ratio of inertial lift to drag forces for the two particle sizes. Images printed from ref. 39 with permission. (B) A spiral channel with a single inlet and two outlets were used for applications in particle filtration. Images reprinted from ref. 40 with permission. (C) A single curved arc also results in particle focusing to a single stream which was collected in a branching outlet. Images reprinted from ref. 37 with permission. (D) Sinusoidally shaped channels with asymmetric curvature were also used to focus particles into parallel streams for applications in high-throughput flow cytometry.<sup>21</sup> (E) Particles flowing through asymmetrically curved channels with a single inlet are shown to differentially focus leading to filtration of larger particles from smaller particles as demonstrated by selective isolation of platelets from diluted whole blood.<sup>36</sup>

selectively enriched over RBCs/WBCs in diluted whole blood by  $\sim 100$ -fold in this system at rates of  $1\ \text{mL/min}$  per channel.

### Future directions of inertial microfluidics

Application of inertial effects at the microscale has only very recently been appreciated as being useful. As such, there is ample critical future research that should be done to further understand and apply these systems to solve a variety of real-world problems. Theoretical models of inertial migration and ordering for example have exciting potential areas for improvement in accuracy and relevance to real samples. First, the current theory, and simplified predictions it makes (Box 1), must be validated with direct experiments. Differences between predictions and experiments will need to be identified to inform future modeling efforts. Effects that will be important to consider in future theoretical models include: (i) the finite-size of particles and how this effects lift forces locally,<sup>19,20</sup> (ii) variations of lift force and secondary flow shape with Reynolds number, (iii) additional deformability-induced lift forces on droplets and cells,<sup>44–46</sup> (iv) interparticle forces and ordering,<sup>26,27</sup> and (v) effects of particle shapes.<sup>21</sup> Theoretical investigation will help inform new system designs for optimal separations of different classes of cells and particles. For example, our recent predictions of particle-size-dependent equilibrium positions in straight channels suggest separation mechanisms based on this effect.<sup>19</sup> Finally, an intuitive understanding of the physical basis of inertial lift forces such that a more general audience can understand the *why* of the particular scaling laws we observe would be useful, and developing this intuition will require further input from fluid mechanicians working together with more applied researchers.

Investigation of new applications for inertial microfluidic phenomena is also very promising. Particle focusing and manipulation technologies naturally fit with applications in flow cytometry and separations, while movement of the fluid itself is of use in opto-fluidics and mixing for Lab-on-a-Chip applications. Integration of inertial focusing with flow cytometry instrumentation has yet to be demonstrated, but is a logical next step given the huge reduction in sheath fluid reagent consumption that is possible. Additionally, new instruments based on massive parallelism will benefit from novel parallel optical detection/imaging technologies. Applications in high-throughput separations still need to be explored, but in most cases I expect them to be focused on macroscale operations on large volumes, not chip-scale separations. Separation/filtration without membranes in industrial and chemical processes, waste-water treatment, emulsion processing, and de-bubbling will be fruitful to explore. Biomedical separations for filtration of blood components, or concentration of cells/bacteria from blood and other bodily fluids such as urine, saliva, and cerebral spinal fluid are other areas of potential research. It should be noted that applications in blood cell separation will require further improvements in size accuracy before becoming practical.

Future commercialization of inertial microfluidic technology appears bright, as demonstrated by the large amount of development initiated for inertial filtration at PARC. Overall, first generation systems operate simply and robustly, further suggesting future commercial success. Notably, these first generation systems have been developed without theoretical guidance and I anticipate improved control and applications as theory begins informing design decisions. Along the same lines as semiconductor physics enabled precision control of electrons, a revolution in inertial fluid physics has the potential to enable



manipulation of fluids, cells, and particles with unprecedented precision, with additional applications that we are only beginning to imagine.

## Acknowledgements

The author would like to acknowledge helpful review, comments, and suggestions from Jon Edd, David Breslauer, and the Microfluidic Biotechnology Lab members.

## References

- 1 T. M. Squires and S. R. Quake, Microfluidics: Fluid physics at the nanoliter scale, *Rev. Mod. Phys.*, 2005, **77**, 977.
- 2 A. P. Sudarsan and V. M. Ugaz, Multivortex micromixing, *Proc. Natl. Acad. Sci. U. S. A.*, 2006, **103**, 7228–33.
- 3 D. Chiu, Cellular manipulations in microvortices, *Anal. Bioanal. Chem.*, 2006, **387**, 17–20.
- 4 S. A. Berger, L. Talbot and L. S. Yao, Flow in curved pipes, *Annu. Rev. Fluid Mech.*, 1983, **15**, 461–512.
- 5 J. Ottino and S. Wiggins, Introduction: mixing in microfluidics, *Philos. Trans. R. Soc. London, Ser. A*, 2004, **362**, 923–935.
- 6 J. Ottino, Mixing, chaotic advection, and turbulence, *Annu. Rev. Fluid Mech.*, 1990, **22**, 207–253.
- 7 R. Liu, M. Stremler, K. Sharp, M. Olsen, J. Santiago, R. Adrian, H. Aref and D. Beebe, Passive mixing in a three-dimensional serpentine microchannel, *J. Microelectromech. Syst.*, 2000, **9**, 190–197.
- 8 P. B. Howell, D. R. Mott, J. P. Golden and F. S. Ligler, Design and evaluation of a Dean vortex-based micromixer, *Lab Chip*, 2004, **4**, 663–9.
- 9 A. P. Sudarsan and V. M. Ugaz, Fluid mixing in planar spiral microchannels, *Lab Chip*, 2006, **6**, 74–82.
- 10 X. Mao, J. R. Waldeisen and T. J. Huang, “Microfluidic drifting” – implementing three-dimensional hydrodynamic focusing with a single-layer planar microfluidic device, *Lab Chip*, 2007, **7**, 1260–2.
- 11 X. Mao, J. R. Waldeisen, B. K. Juluri and T. J. Huang, Hydrodynamically tunable optofluidic cylindrical microlens, *Lab Chip*, 2007, **7**, 1303–8.
- 12 D. H. Yoon, J. B. Ha, Y. K. Bahk, T. Arakawa, S. Shoji and J. S. Go, Size-selective separation of micro beads by utilizing secondary flow in a curved rectangular microchannel, *Lab Chip*, 2009, **9**, 87–90.
- 13 G. Segre and A. Silberberg, Radial Particle Displacements in Poiseuille Flow of Suspensions, *Nature*, 1961, **189**, 209–210.
- 14 R. G. Cox and H. Brenner, The lateral migration of solid particles in Poiseuille flow – I theory, *Chem. Eng. Sci.*, 1968, **23**, 147–173.
- 15 B. P. Ho and L. G. Leal, Inertial Migration of Rigid Spheres in Two-Dimensional Unidirectional Flows, *J. Fluid Mech.*, 1974, **65**, 365–400.
- 16 J. A. Schonberg and E. J. Hinch, Inertial Migration of a Sphere in Poiseuille Flow, *J. Fluid Mech.*, 1989, **203**, 517–524.
- 17 E. S. Asmolov, The Inertial Lift on a Spherical Particle in a Plane Poiseuille Flow at Large Channel Reynolds Number, *J. Fluid Mech.*, 1999, **381**, 63–87.
- 18 J. Matas, J. F. Morris and E. Guazzelli, Inertial Migration of Rigid Spherical Particles in Poiseuille Flow, *J. Fluid Mech.*, 2004, **515**, 171–195.
- 19 D. Di Carlo, J. F. Edd, K. J. Humphry, H. A. Stone and M. Toner, Particle Segregation and Dynamics in Confined Flows, *Phys. Rev. Lett.*, 2009, **102**, 094503–4.
- 20 J. Matas, J. F. Morris and E. Guazzelli, Lateral Force on a Rigid Sphere in Large-Inertia Laminar Pipe Flow, *J. Fluid Mech.*, 2009, **621**, 59–67.
- 21 D. Di Carlo, D. Irimia, R. G. Tompkins and M. Toner, Continuous inertial focusing, ordering, and separation of particles in microchannels, *Proc. Natl. Acad. Sci. U. S. A.*, 2007, **104**, 18892–7.
- 22 B. Chun and A. J. C. Ladd, Inertial migration of neutrally buoyant particles in a square duct: An investigation of multiple equilibrium positions, *Phys. Fluids*, 2006, **18**, 031704–4.
- 23 A. A. S. Bhagat, S. S. Kuntaegowdanahalli and I. Papautsky, Enhanced particle filtration in straight microchannels using shear-modulated inertial migration, *Phys. Fluids*, 2008, **20**, 101702–4.
- 24 Y. W. Kim and J. Y. Yoo, The lateral migration of neutrally-buoyant spheres transported through square microchannels, *J. Micromech. Microeng.*, 2008, **18**, 065015.
- 25 J. F. Edd, D. Di Carlo, K. J. Humphry, S. Köster, D. Irimia, D. A. Weitz and M. Toner, Controlled encapsulation of single-cells into monodisperse picolitre drops, *Lab Chip*, 2008, **8**, 1262–4.
- 26 J. Matas, V. Glezer, E. Guazzelli and J. F. Morris, Trains of particles in finite-Reynolds-number pipe flow, *Phys. Fluids*, 2004, **16**, 4192–4195.
- 27 Y. Yan, J. F. Morris and J. Koplik, Hydrodynamic interaction of two particles in confined linear shear flow at finite Reynolds number, *Phys. Fluids*, 2007, **19**, 113305–12.
- 28 T. Inamuro, K. Maeba and F. Ogino, Flow between parallel walls containing the lines of neutrally buoyant circular cylinders, *Int. J. Multiphase Flow*, 2000, **26**, 1981–2004.
- 29 Z. Wu, B. Willing, J. Bjerketorp, J. K. Jansson and K. Hjort, Soft inertial microfluidics for high throughput separation of bacteria from human blood cells, *Lab Chip*, 2009, **9**, 1193–1199.
- 30 J. Park, S. Song and H. Jung, Continuous focusing of microparticles using inertial lift force and vorticity via multi-orifice microfluidic channels, *Lab Chip*, 2009, **9**, 939–948.
- 31 P. S. Williams, S. H. Lee and J. C. Giddings, Characterization of hydrodynamic lift forces by field-flow fractionation – inertial and near-wall lift forces, *Chem. Eng. Commun.*, 1994, **130**, 143–166.
- 32 P. S. Williams, M. H. Moon and J. C. Giddings, Influence of accumulation wall and carrier solution composition on lift force in sedimentation/steric field-flow fractionation, *Colloids Surf., A*, 1996, **113**, 215–228.
- 33 P. S. Williams, M. H. Moon, Y. Xu and J. C. Giddings, Effect of viscosity on retention time and hydrodynamic lift forces in sedimentation/steric field-flow fractionation, *Chem. Eng. Sci.*, 1996, **51**, 4477–4488.
- 34 J. A. Levesley and B. J. Bellhouse, Particulate separation using inertial lift forces, *Chem. Eng. Sci.*, 1993, **48**, 3657–3669.
- 35 D. R. Gossett and D. Di Carlo, Particle focusing mechanisms in curving confined flows, *Anal. Chem.*, 2009, DOI: 10.1021/ac901306y.
- 36 D. Di Carlo, J. F. Edd, D. Irimia, R. G. Tompkins and M. Toner, Equilibrium separation and filtration of particles using differential inertial focusing, *Anal. Chem.*, 2008, **80**, 2204–11.
- 37 N. Oozeki, S. Ookawara, K. Ogawa, P. Lob and V. Hessel, Characterization of Microseparator/Classifier with a Simple Arc Microchannel, *AIChE J.*, 2009, **55**, 24–34.
- 38 J. Seo, M. H. Lean and A. Kole, Membrane-free microfiltration by asymmetric inertial migration, *Appl. Phys. Lett.*, 2007, **91**, 033901–3.
- 39 A. A. S. Bhagat, S. S. Kuntaegowdanahalli and I. Papautsky, Continuous particle separation in spiral microchannels using Dean flows and differential migration, *Lab Chip*, 2008, **8**, 1906–14.
- 40 J. Seo, M. H. Lean and A. Kole, Membraneless microseparation by asymmetry in curvilinear laminar flows, *J. Chromatogr., A*, 2007, **1162**, 126–31.
- 41 “Industrial Liquid Filtration - PARC (Palo Alto Research Center)”. <http://www.parc.com/work/focus-area/industrial-liquid-filtration/>, accessed August 11, 2009.
- 42 S. S. Kuntaegowdanahalli, A. A. S. Bhagat and I. Papautsky, Inertial microfluidics for continuous particle separation in spiral microchannels, *Lab Chip*, 2009, DOI: 10.1039/b908271a.
- 43 A. Russom, A. K. Gupta, S. Nagrath, D. Di Carlo, J. F. Edd and M. Toner, Differential inertial focusing of particles in curved low-aspect-ratio microchannels, *New J. Phys.*, 2009, **11**, 075025.
- 44 P. C. Chan and L. G. Leal, The Motion of a Deformable Drop in a Second-Order Fluid, *J. Fluid Mech.*, 1979, **92**, 131–170.
- 45 C. K. W. Tam and W. A. Hyman, Transverse Motion of an Elastic Sphere in a Shear Field, *J. Fluid Mech.*, 1973, **59**, 177–185.
- 46 Y. Zhao and M. K. Sharp, Finite Element Analysis of the Lift on a Slightly Deformable and Freely Rotating and Translating Cylinder in Two-Dimensional Channel Flow, *J. Biomech. Eng.*, 1999, **121**, 148–152.